

1                   **Some Methods for Addressing Errors in Static AIS Data Records**

2                   Steven D. Meyers<sup>\*a</sup>, Yasin Yilmaz<sup>b</sup> and Mark E. Luther <sup>a</sup>

3                                   <sup>a</sup>*Center for Maritime and Port Studies*  
4   *University of South Florida,*  
5   *St. Petersburg, FL, USA*  
6                                   smeyers@usf.edu, mluther@usf.edu

7                                   <sup>b</sup>*College of Engineering*  
8   *University of South Florida,*  
9   *Tampa, FL, USA*  
10                                   yasiny@usf.edu

11   \*corresponding author

12  
13                                   **Abstract**

14   The Automatic Identification System (AIS) provides essential services in support of maritime  
15   domain awareness. Accurate AIS values for hull dimension and type are often critical for safe  
16   and efficient management of ship traffic, and for development of new artificial intelligence  
17   maritime algorithms. AIS variables are subject to fault from multiple sources, ranging from bad  
18   weather to human error. New heuristic methods for correcting ship draft, beam, and class were  
19   developed and evaluated, using AIS data in the vicinity of large Florida ports as a test bed. Novel  
20   low order polynomials for 9 broad functional vessel classes yielded predicted values for draft and  
21   beam as functions of vessel length. The majority of relative differences between predicted and  
22   reported values were <0.1. A logistic regression (LR) multiclass classification scheme using the  
23   residuals from these polynomial predictions generally showed good agreement between  
24   estimated and reported vessel class. The LR scheme demonstrated skill in verifying AIS-  
25   transmitted classification, detecting incorrectly classified vessels, and flagging those with  
26   incorrect draft or operating near an extreme draft. A diagnostic of reports whose classification  
27   had very low and very high confidence suggested directions for further improvement of the  
28   algorithm. A new hierarchy for processed AIS data is proposed.

29  
30  
31  
32  
33   Keywords: automatic identification system; multiclass classification; vessel identification;  
34   logistic regression; maritime domain awareness

## 35 Introduction

36 The Automatic Identification System (AIS) is a maritime vessel recognition scheme originally  
37 designed to increase situational awareness between vessels, and between vessels and ports  
38 (Harre, 2000; Murk, 1999). Through the AIS, vessels transmit their identifying information every  
39 few minutes using automated radio signals. Two general categories of data are provided by the  
40 AIS: static and dynamic. Static variables are typically fixed quantities, including the Maritime  
41 Mobile Service Identity (MMSI) number, length ( $L$ ), beam ( $B$ ), draft ( $D$ ), and type ( $Y$ ), though  
42 the draft of cargo and tanker ships can change when material is offloaded or unloaded. Crew  
43 members are responsible for entering the static values into the AIS transmitter. Dynamic  
44 variables include time of transmission, vessel position, speed over ground, and heading. These  
45 are typically entered into the report automatically by instrumentation.

46 AIS data can be accessed in real-time using specialized receivers that pickup broadcasts within a  
47 ~50 km radius, or with a slight delay through data service companies such as Pole Star USA,  
48 Marine Traffic, GateHouse Maritime, and others that access the ground-based as well as satellite  
49 AIS receivers. These companies often provide small amount of AIS data to researchers without  
50 charge. Processed AIS data in US coastal waters is also available, sometimes with a significant  
51 delay but without cost, from Marine Cadastre ([marinecadastre.gov/ais](http://marinecadastre.gov/ais)), a combined service of  
52 the U.S. Department of Commerce's National Oceanic and Atmospheric Administration  
53 (NOAA) Office for Coastal Management and the U.S. Department of the Interior's Bureau of  
54 Ocean Energy Management (BOEM). Regardless of the provider, most of these data are offered  
55 with little to no error flagging or correction. This may be because objective error handling  
56 routines for AIS data are still under development, most of which have focused on the dynamic  
57 variables. There have been few publications regarding the static AIS variables in this context.  
58 Adoption of a standard set of handling routines would facilitate AIS usage in a range of  
59 applications. The outline for such a system is proposed at the end of this article.

60 AIS data have become essential to the monitoring and management of global vessel traffic, as  
61 well as in academic and private sector maritime research programs (Tu et al., 2017; Yang et al.,  
62 2019). The latter encompasses many areas of maritime operations, including relatively simple  
63 maps of vessel traffic density (Demšar and Virrantaus, 2010; Shelmerdine, 2015), predicting  
64 future routes and collision avoidance (Chen et al., 2018; Rong et al., 2019; Silveira et al., 2013;  
65 Wang et al., 2013), predicting arrival times (Dobrkovic et al., 2016; Jahn and Scheidweiler,  
66 2018; Xin et al., 2019), and detecting anomalous vessel movement (Liu, 2015; Oh et al., 2018;  
67 Sidibé and Shu, 2017). Lim et al. (2018), Robards et al. (2016), and Zhou et al. (2019) provide  
68 reviews of AIS applications, many of which utilize artificial intelligence / machine learning  
69 where AIS records are used as a source of training data.

70 Incomplete or inaccurate AIS reports can confound studies of maritime operation. Such faulty  
71 data arise from multiple causes, such as human error, instrument failure, an overwhelmed  
72 transmission spectrum, and atmospheric interference (Emmens et al., 2021; Harati-Mokhtari et

73 al., 2007). Processed AIS data may also be subject to  
74 errors or inconsistencies in sorting, filtering, or  
75 transcription. Most previous studies have focused on  
76 detection of dynamic AIS errors (Bošnjak et al., 2012;  
77 Sun et al., 2021; Zhao et al., 2018). Of relevance to  
78 this study, Guo et al. (2021) used kinematically-based  
79 cubic polynomials to model trajectories and determine  
80 errors in vessel position and speed by their generic  
81 “distance” from the model. There have been few  
82 publications that focused on correcting static AIS  
83 errors. Wang et al. (2021) applied the Random Forest  
84 algorithm to AIS static values to identify five vessel  
85 classes. Sheng et al. (2018) developed a logistic  
86 regression binary classifier that discriminated between  
87 Cargo and Fishing class vessels based on their  
88 position, course, and speed near Shantou, China.  
89 Steidel et al. (2019) suggested correcting AIS  
90 Destination data using a combination of automated and  
91 direct communication with each vessel. Atypical B vs.  
92 L values were used to manually identify 3  
93 misclassified, misreported, or unusually large vessels  
94 in a narrowly defined group of bulk carriers (Smestad  
95 et al., 2017).



Figure 1. Map of peninsular Florida. The 5 largest ports are indicated.

96 This study examines some novel methods for correcting errors in static variables associated with  
97 hull dimension and type for many vessel classes. As demonstrated below, these variables were  
98 found to be interrelated and could be used to help determine missing values or detect  
99 inconsistencies in the group of values for many vessels. The methods examined start with simple  
100 heuristic drop-out replacement, but also include a new algebraic representation that takes  
101 advantage of the dependence between the static variables related to hull geometry, and a  
102 multiclass classification (MCC) scheme for confirming functional vessel class. The methods  
103 developed here can be used to flag or correct some missing or unusual static AIS variables.

104 Section 2 describes the AIS data used in this study. Restricting the analysis to underway vessels  
105 in the vicinity of large Florida ports (Figure 1) reduced computational cost for this initial analysis  
106 while retaining diversity of vessel types. Polynomial models and logistic regression are described  
107 as they relate to this study. Section 3 presents the geometric relations of hull dimensions found  
108 when partitioning by vessel functional class. The number of missing or inconsistent static values  
109 is then examined, and the potential use of polynomials to represent geometric hull relations and  
110 correct these errors is tested. This is followed by the development and testing of the new vessel

111 classification system. Section 4 is a Discussion of the findings and how the methods employed  
112 might be adapted or improved. A new system of organizing processed AIS data is proposed.

113

## 114 2. Data and Methods

### 115 2.1 AIS Data

116 The AIS is divided into Class A and Class B. Class A transmissions have a range around 30-50  
117 km, are prioritized by the system, and are mandatory for large and passenger vessels subject to  
118 the International Convention for the Safety of Life at Sea (SOLAS). Class B transmissions have  
119 a range ~16 km, are not prioritized, and are used by non-SOLAS craft, typically personal  
120 watercraft and some smaller, domestic commercial vessels.

121 AIS reports for the years 2015-2019 were obtain from Marine Cadastre who added Class B to  
122 their AIS records starting in 2018. Years prior only contained Class A reports. Also prior to  
123 2018,  $L$  and  $B$  were provided to a precision of 0.01 m, but afterwards were provided as integer  
124 values. A relatively small subset of these reports was utilized in this analysis to facilitate  
125 development of the algorithms presented in this study.

126 Following Mitchell and Scully (2014), irregular polygonal Areas of Interest (AOI) around the  
127 five largest commercial ports in the state of Florida, Miami, Everglades, Jacksonville, Tampa,  
128 and Palm Beach, (Figure 1), were used to delimit a subset of AIS records. Vessel traffic is  
129 concentrated around ports. Extracting AIS records near them reduces the volume of records to be  
130 examined while retaining a breadth of sample comparable to that obtained from larger areas  
131 (e.g., the entire coast of Florida) that would include many of the same vessels as they traveled  
132 between ports. Each AOI included the port and its access waters and channels. AIS reports from  
133 all the ports were binned and analyzed collectively. Vessels that were slow or not moving (speed  
134  $< 0.5$  kn) for an entire year were not considered. This yielded a nominal  $10^7$  AIS reports per year  
135 of which  $< \sim 0.01\%$  lacked an MMSI, and were removed from the analysis. Some of the reports  
136 with missing MMSI provided an IMO number which could have been be used to check the  
137 vessel identification using an external database (Winkler, 2012), but the focus here was on  
138 exploiting relations between the geometric static values.

139 The unique MMSI and associated values of  $L$ ,  $D$ ,  $B$ , and  $Y$  reported in the AIS were determined.  
140 The number of vessels by class, and the number of vessels in each class with problems in their  
141 statics were found. For example, the number of vessels reporting both  $D = 0$  and  $D > 0$  (at  
142 different times) provided a measure of the utility for a direct replacement method. Calculating  
143 this same number but restricted to  $L > 30$  m, eliminated many personal craft that have a higher  
144 rate of static AIS errors (Meyers et al., 2020), and helped focus the analysis on commercial and  
145 other ships more likely to be professionally maintained.

146

147 2.2 Functional Vessel Classes

148 Vessel identification in the AIS includes a choice from about 100 unique numbers that indicate  
 149 vessel type such as search and rescue, recreational, cargo, and tanker, with the latter two further  
 150 divided into a general type or one of several hazard classifications. Marine Cadastre organizes  
 151 many of these AIS types into functional classes. A similar prescription was followed here, with  
 152 each AIS report being labeled according to the class for the reported type (Table 1). About 10-  
 153 15% of the vessels were not readily incorporated into a functional class (e.g., types 1005, 1007,  
 154 1018), so were not part of the class-based analysis. The number of unique vessels within each  
 155 class was determined for each year 2015-2019 (Tables 2, 3). Large year over year changes in the  
 156 relative number of vessels for some classes appear to have been associated with changes in the  
 157 processing of the AIS data provided by Marine Cadastre. For example, in 2018 several Supply  
 158 class vessels started reporting as type 90, which is ‘unspecified’, decreasing the number in the  
 159 class. Similarly, many pilot and tender vessels made the opposite switch in 2018, changing from  
 160 an unspecified type to one that fit within the Enforcement class as defined here, though most of  
 161 these were smaller vessels ( $L < 30$  m) so did not impact the bulk of the analysis. Additionally, a  
 162 small number of military vessels became identifiable as such in 2018 before which they were  
 163 typically listed as ‘public’ or ‘other’ AIS types.

164 Table 1. AIS types in defined functional vessel classes, and the number of unique vessels in each class by  
 165 year.

<b><u>Class</u></b>	<b><u>AIS Vessel Type</u></b>	<b><u>2015</u></b>	<b><u>2016</u></b>	<b><u>2017</u></b>	<b><u>2018</u></b>	<b><u>2019</u></b>
<b>Recreational</b>	36,37,1019	3011	3595	3858	5953	6596
<b>Cargo</b>	70-79,1003,1004,1016	1263	1306	1266	1189	1129
<b>Tug</b>	21,22,31,32,52,1023,1025	342	373	395	404	373
<b>Tanker</b>	80-89, 1017, 1024	303	262	244	218	212
<b>Passenger</b>	60-69, 1012-1015	171	212	245	260	263
<b>Fishing</b>	30,1001,1002	51	1025	158	211	224
<b>Supply</b>	1010	28	34	42	0	0
<b>Research</b>	1020	24	22	24	0	0
<b>Enforcement</b>	35,50,53,55	0	2	3	39	55

166

167 It was useful to define the set of all AIS reports ( $A$ ) such that  $L, B, D$ , and  $Y$  are positive, real-  
 168 valued numbers. That is, the set  $A = \{k: L_k, B_k, D_k, Y_k > 0\}$ , where  $k$  indexes the reports.  
 169 Further, subsets of  $A$  for a particular class  $c$ ,  $S_c = \{A: Y \in c\}$  and its complement  $S'_c = \{A: Y \notin c\}$   
 170 were defined.

171

172

173 Table 2. Total numbers by year: Number of unique MMSI, number with only zero or missing values for  
 174 the indicated static variable, number with multiple *D*, number with multiple *D* including at least one zero  
 175 value, number with all hull dimensions but undefined type.

	<b><u>2015</u></b>	<b><u>2016</u></b>	<b><u>2017</u></b>	<b><u>2018</u></b>	<b><u>2019</u></b>
# Unique Vessels	6728	7561	8428	9052	9838
# all <i>L</i> =0	1449	1928	2843	2220	2263
# all <i>D</i> =0	4310	5327	6401	6924	7827
# all <i>B</i> =0	3178	3931	4808	4017	3899
# all <i>Y</i> =0	1378	581	1994	487	683
# Multiple <i>D</i>	147	883	523	118	99
# Multiple w/ <i>D</i> =0	9	846	491	25	10
# <i>LBD</i> >0 & <i>Y</i> =0	42	6	28	10	11

176

177

178 Table 3. Same as Table 2 but restricted to *L*>30 m.

	<b><u>2015</u></b>	<b><u>2016</u></b>	<b><u>2017</u></b>	<b><u>2018</u></b>	<b><u>2019</u></b>
# Unique Vessels	2472	2520	2468	2422	2371
# all <i>D</i> =0	244	451	562	464	508
# all <i>B</i> =0	80	181	185	177	180
# all <i>Y</i> =0	51	3	24	16	17
# Multiple <i>D</i>	136	804	474	93	91
# Multiple w/ <i>D</i> =0	4	768	443	5	3
# <i>LBD</i> >0 & <i>Y</i> =0	5	1	4	4	6

179

### 180 2.3 Replacement Methods for Static AIS

181 The 2018 change in some AIS types suggested a simple method for improving the accuracy of  
 182 static descriptors for a vessel. If a static AIS variable is accepted as valid during one time period,  
 183 but provides a different, invalid or missing value during another time, then the valid value can be  
 184 used to replace the values in question. This was the first method assessed in this study.

185

186

187 Table 4. Quadratic fitting for each class (Table 1) beam and draft, based on 2015-2019 AIS records.  
 188 Shown are the class name, maximum AIS vessel length value in class ( $L_{max}$ ), the extrema vessel length  
 189 ( $L_{ex}$ ), fitting coefficients (1), number of unique vessels used in the fit ( $N$ ), the root-mean-square  
 190 difference between estimated and actual values in the fit (RMSD), and the mean relative absolute  
 191 difference (MRAD) of the fit.

Class	$L_{max}$ (m)	$L_{ex}$ (m)	$c_2$ ( $10^{-4} m^{-1}$ )	$c_1$	$c_0$ (m)	N	RMSD (m)	MRAD
<b>Beam</b>								
Cargo	200	-46.9	4.15	0.0389	8.16	2198	1.906	0.058
Tanker	200	-159.3	3.03	0.0965	3.35	576	1.697	0.047
Passenger	199	188.1	-6.80	0.2570	0.75	67	3.052	0.141
Tug	180	197.9	-4.60	0.1808	5.03	379	2.783	0.101
Fishing	40	58.3	-20.5	0.2386	1.90	36	1.059	0.136
Recreational	163	-707.7	0.84	0.1187	3.33	667	1.335	0.089
Research	126	18.1	21.4	-0.0775	9.64	35	4.012	0.142
Supply	130	30.2	12.4	-0.0746	15.48	46	4.608	0.153
<b>Draft</b>								
Cargo	367	366.4	-1.10	0.0812	-1.21	3048	1.408	0.125
Tanker	337	390.2	-1.40	0.1069	-3.27	718	1.405	0.101
Passenger	362	498.4	-0.35	0.0353	0.94	182	0.593	0.094
Tug	180	118.0	7.00	0.1651	-0.29	379	0.996	0.148
Fishing	40	14.4	-2.70	0.0079	2.60	36	0.616	0.191
Recreational	163	-6.1	2.31	0.0028	2.13	667	0.870	0.201
Research	126	145.9	-4.20	0.1225	-1.36	35	0.706	0.164
Supply	130	145.4	-5.20	0.1519	-2.97	46	0.633	0.110

192  
 193 The second method was developed to fill missing  $B$  and  $D$  values when no such replacement  
 194 value is available, and to potentially detect faulty values of these variables. Hull aspect ratios  
 195 such as  $D/L$  are often selected by marine engineers to maximize operational performance  
 196 (Bertram and Schneekluth, 1998; Papanikolaou, 2014; Zhang et al., 2008), and therefore often  
 197 vary in a consistent way within a functional class. The dependence of beam  $B(L)$  and draft  $D(L)$   
 198 on length for each class were represented using  $n$ -degree polynomials with independent variable  
 199  $L$  as

$$\phi_n(L) = c_0 + \sum_{i=1}^n c_i L^i \quad (1)$$

200  
 201 where the constants  $c_i$  were determined through standard least-squares (Table 4). A minimum of  
 202 10 independent  $(L, S)$  pairs for each class were required for the estimate, where  $S$  represented the

203 static value  $B$  or  $D$  being modeled. Changes in vessel draft due to changes in deadweight tonnage  
 204 were not represented by (1). Bulk measures of the accuracy of (1) compared to values from AIS  
 205 were root mean square difference (RMSD)

$$\sqrt{\frac{1}{N_c} \sum_{k=1}^{N_c} (\phi_n(L_k) - S_k)^2} \quad (2)$$

206

207 and mean relative absolute difference (MRAD)

$$\frac{1}{N_c} \sum_{k=1}^{N_c} \frac{|\phi_n(L_k) - S_k|}{S_k} \quad (3)$$

208

209 where  $L_k$  is the  $k$ -th AIS length value in class  $c$ ,  $S_k$  is the matching static value, and  $k=1, \dots, N_c$ .  
 210 The relation between  $(\phi_n(L_k) - S_k)/S_k$  and  $L_k$  was also examined to further evaluate this  
 211 method of estimating static values.

212

## 213 2.4 Multiclass Classification

214 Logistic regression (LR) is widely used to represent a dichotomous (2-valued) variable ( $y$ ) that  
 215 has a single transition between one value and the other (generally 0 and 1), dependent upon  
 216 predictor variables  $\mathbf{X}$  (Hilbe, 2016; Hosmer Jr et al., 2013). Here LR was used to identify vessels  
 217 according to their functional class. Basic LR models the odds ratio of probability  $0 \leq \pi \leq 1$  for  
 218  $y=1$  as

$$\ln\left(\frac{\pi}{1-\pi}\right) = \beta_0 + \sum_{i=1}^{N_v} \beta_i X_i = \boldsymbol{\beta} \cdot \mathbf{X} \quad (4)$$

219 where  $\mathbf{X}$  is a set of  $N_v$  independent variables (alternatively called covariates or predictors), and  $\boldsymbol{\beta}$   
 220 is a vector of coefficients. In this application, the predictors were the difference between the  
 221 AIS-reported values of draft and beam and those predicted from (1). Inverting (4) yields the  
 222 probability

$$\pi(y = 1|\mathbf{X}) = \frac{\exp(\boldsymbol{\beta} \cdot \mathbf{X})}{1 + \exp(\boldsymbol{\beta} \cdot \mathbf{X})} \quad (5)$$

223

224 In practice, a set of data  $\mathcal{D} = \{\mathbf{X}, y\}$  of index  $k = 1, \dots, n$ , is divided according to the value of  $y$   
 225 into two sets of size  $n_0$  and  $n_1$ , respectively. The  $\boldsymbol{\beta}$  are then determined, usually by maximizing  
 226 the log-likelihood function



$$\arg \max_{\beta} \sum_{i=1}^n [y_i \log \pi_i + (1 - y_i) (1 - \log \pi_i)] \quad (6)$$

227

228 where the  $\pi_i$  carry the  $\beta$ -dependence. A common issue that must often be addressed is  
 229 unbalanced data, when  $n_0 \gg n_1$ , or the reverse, which can bias (6), resulting in poor estimates of  
 230 the coefficients and degrade the fidelity of the model. See King and Zeng (2001) and Salas-  
 231 Eljatib et al. (2018) for additional details. A similar issue arises when  $\mathcal{D}$  contains clusters around  
 232 one or more points in the data space (Merlo et al., 2006). Defining a subset of  $\mathcal{D}$  using random  
 233 subsampling is often employed in the case of unbalanced data, whereas Tomek Link, Synthetic  
 234 Minority Oversampling, and Neighborhood Cleaning are common solutions to clustered data  
 235 (Elhassan and Aljurf, 2016; Guo and Wei, 2019). In this study, random subsampling was used to  
 236 address the data imbalance as there was little clustering in the data.

237

238 LR can also be used to represent the probabilistic choice between two distinct quantities based  
 239 on the same independent variables. Here we examined the probability of vessels being in class  $c$   
 240 compared to the probability of the vessel belonging to any other class  $c'$ ,

$$\ln \left( \frac{\pi(c | \delta, \gamma)}{\pi(c' | \delta, \gamma)} \right) = \beta_c \cdot X \quad (7)$$

241

242 given the parameters  $\delta$  and  $\gamma$  related to the residuals of (1), defined below. Similar “one-vs-rest”  
 243 classification schemes (Bisong, 2019) have been applied to a variety of labels, including cancer  
 244 diagnosis (Zhu and Hastie, 2004), handwriting analysis (Klimaszewski, 2015), and astronomical  
 245 redshift (Stivaktakis et al., 2019).

246

247 The result of LR (5) is a real value in the range [0,1]. A threshold probability value is typically  
 248 defined such that if  $\pi < \pi_0$  then  $y$  is considered to equal 0, and  $y=1$  when  $\pi \geq \pi_0$ . The most  
 249 common selection for this threshold is  $\pi_0=0.5$ , but this is somewhat arbitrary. In this study  $\pi_0$   
 250 was allowed to vary, and the resulting changes in the rate of true positive (TPR) vessel  
 251 classifications, and the rate of false Positive (FPR) classifications were found for each class,  
 252 assuming the AIS-reported vessel type was correct. These were used to construct Receiver  
 253 Operating Characteristic (ROC) curves, defined as TPR vs. FPR on the unit square, and the Area  
 254 Under Curve (AUC) of the ROC (Fawcett, 2006; Huang and Ling, 2005). ROC curves in  
 255 proximity to the upper-left corner of the domain (high TPR, low FPR) are have higher fidelity.  
 256 Values of AUC range from 0 to 1, with the higher values generally considered an indication of  
 257 an accurate classification scheme. An AUC value of 0.5 indicates even probability of TP and FP,  
 258 essentially random classification.

259

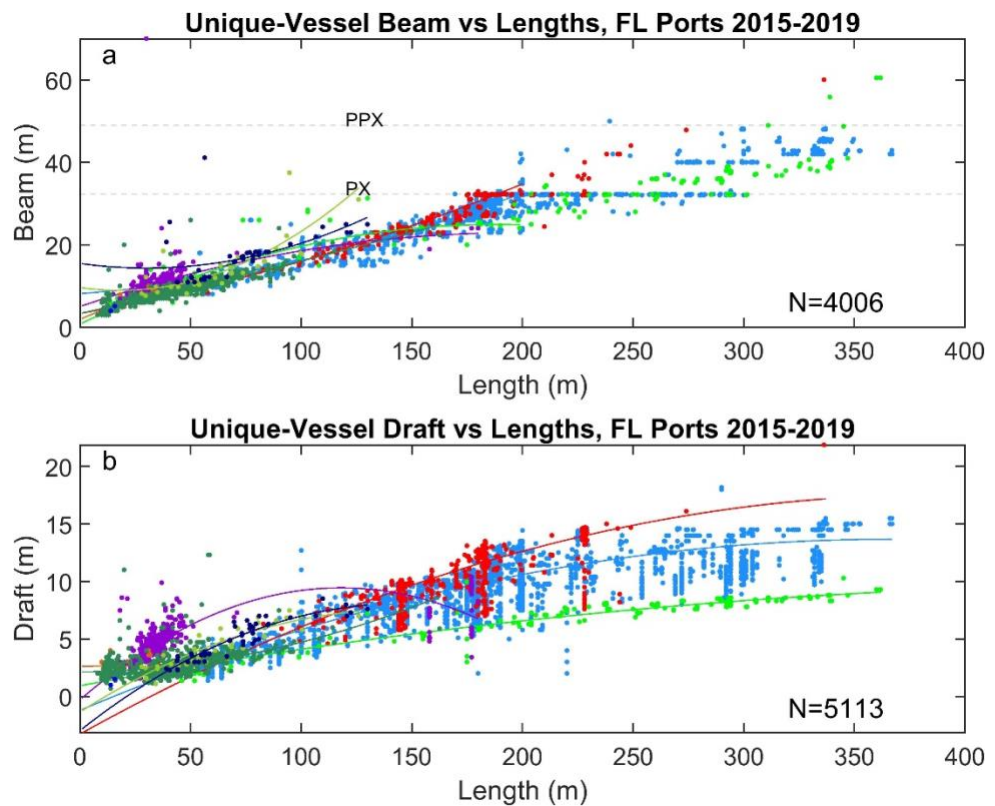
260

261 3. Results

262 The vessel class with the highest number of unique vessels was the Recreational class (Table 1).  
263 From 2015 to 2019 the total number of Recreational vessels roughly doubled after Marine  
264 Cadastre started reporting class-B AIS in 2018. The number of reported Fishing vessels spiked in  
265 2016. This is also likely to again be due to changes in reporting. During that same time period  
266 the number of Tanker vessels decreased by almost 1/3, but this was likely due to a change in  
267 operations, not reporting. Overall, the total number of vessels roughly doubled (Table 2), with  
268 most of that due to an increase in the number of small ( $L < 30$  m) vessels. The total number of  
269 larger vessels showed a weak trend, decreasing from 2520 in 2016 to 2371 in 2019.

270 3.1 Hull Dimensions

271 Scatter plots of the  
272 hull dimensions  
273 illustrate how the  
274 dependence of  
275 vessel beam  $B(L)$   
276 and draft  $D(L)$   
277 varied by class  
278 (Figure 2), with  
279 both generally  
280 increasing with  $L$ .  
281 There was little  
282 class difference  
283 apparent for  $B(L)$ .  
284 For  $L < \sim 200$  m,  $B$   
285 increased roughly  
286 linearly with  $L$  for  
287 all classes. Tug and  
288 Supply class vessels  
289 had the largest beam



290 Figure 2. (a) Unique-vessel beam vs length, by functional class (Table 1). Dashed  
291 lines indicate Panamax beam (PX) and Post-Panamax (PPX) beam sizes. Number  
292 of vessels ( $N$ ) with both  $L, Y > 0$  and  $0 < B \leq 200$  m is indicated. (b) Unique-vessel  
293 draft vs length, coded by functional class. Solid lines are quadratic fits for each  
294 class. Number of vessels with  $L, D, B, Y > 0$  is indicated.

295  $B$  by design. Many of these ships have been in operation for years and were built to pass through  
296 the Panama Canal, so had  $B$  capped at the “Panamax” limit of 32.31 m, in place since the  
297 opening of the canal in 1914. Vessels at or just below this beam size were found for, roughly,  
298 170 m  $< L < 300$  m. In 2016 the Panama Canal expanded the maximum permissible vessel beam  
299 to 51.25 m (“PostPanamax”). Ships with  $B > 32$  m were exclusively Passenger, Tanker, and

300 Cargo class with  $L > 200$  m (Figure 2), though their voyage may not have necessarily included  
301 passage through the Panama Canal.

302 In contrast,  $D(L)$  showed more separation by class (Figure 2). Tugs had the highest nominal rate  
303 of increasing  $D$  with  $L$ , and Passenger class the lowest, though Tugs were generally limited to  
304  $L < \sim 60$  m. The Cargo class included the largest  $L$  reported. Tankers often had the highest  $D$  for a  
305 given  $L$  in their range, and Cargo class generally had drafts between those of Tankers and  
306 Passenger classes for  $L \gtrsim 100$  m. There was less apparent distinction between the classes in the  
307 range  $D \lesssim 3$  m and  $L \lesssim 60$  m.

### 308 3.2 Static Errors

309 The quality of the static data was measured by the number of vessels with missing or conflicting  
310 static values. The unique MMSIs in the study region each year were first identified. Then the  
311 reported values for the static variables of every vessel were determined each year. All vessels  
312 examined reported a single value for  $L$ ,  $B$ , or  $Y$ . About 1-10% of all vessels, depending on the  
313 year, had multiple  $D$  values (Table 2), with up to 24 unique values for a single vessel in one year.  
314 A high percentage of vessels reported zero (or were missing) values for  $L$ ,  $B$ ,  $Y$ , or  $D$ , with  $D$   
315 having the highest rate of zero, reaching  $\sim 80\%$  in 2019. The number of vessels reporting at least  
316 one  $D = 0$  and at least one  $D > 0$  over the same year fluctuated, peaking in 2016 at just under  
317 12% of vessels, and declining to  $\sim 1\%$  in 2019. These rapid changes in quality may be indicative  
318 of changes to the handling of the AIS data, rather than changes in the raw AIS data themselves.  
319 The static error rates were lower for vessels with  $L > 30$  m (Table 3). For example, only about  
320 10-20% of vessels failed to report any  $D$  value in a given year.

321 Individual AIS reports with a missing or zero static value, and a nonzero value for the same  
322 vessel in another report, can be easily corrected by filling the missing value with the nonzero  
323 value. Most static values were unchanging, so a single non-zero value would be sufficient.  
324 However, in the case where multiple  $D$  are available, the choice needs to be judicious, or some  
325 level of acceptable error needs to be determined based on the application.

326 Those vessels entirely missing a static variable, or those without an historical record on which to  
327 draw, require another method for correction. A simple method for estimating  $D(L)$  was therefore  
328 tested. The first step was to identify those MMSI with a complete set of static variables, and then  
329 implement (1) with  $n=2$  for each class of ships with at least 10 unique  $(L, D)$  value pairs per  
330 class. All classes except Enforcement class met these qualifications. The minimum count of ten  
331 was somewhat arbitrary, but helped avoid fitting too sparsely represented classes.

332

### 333 3.3 Polynomial Correction

334 Beam size could only reasonably be represented by a polynomial for  $L < \sim 200$  m, above which  
335 Panamax restrictions dominated the distribution of vessel beam sizes (Figure 2). Just over 4000

336 total vessels with complete static AIS data were partitioned by functional class and their beam  
 337 estimated using (1). The most abundant vessel class was Cargo, with about 2200 unique vessels  
 338 identified (Table 4). Tanker, Passenger, and Tug classes all had several hundred unique vessels;  
 339 all other classes contained a few dozen unique vessels.

340 Differences between the estimated beam ( $B_2$ ) and the beam from AIS ( $B$ ) were found for each  
 341 year, and were generally small. For example, in 2017, 66% of the residual values  $\gamma = |B_2 - B| <$   
 342 1 m, and 89% were  $< 2$  m (Figure 3). A smaller number of much larger  $\gamma$  were found in all  
 343 classes. The relative difference  $r_B = \gamma/B$  was usually higher for smaller ( $L < \sim 75$  m) vessels.

344 With the exception  
 345 of a few outliers, the  
 346 highest  $r_B$  was  $\sim 0.8$ -  
 347 1.0, found near  
 348  $L \sim 10$  m. Overall,  
 349 about 63% of the  
 350 values had  
 351  $\gamma/B < 0.1$ , and about  
 352 90% had  $\gamma/B < 0.25$ .

353 These percentages  
 354 decreased in 2018  
 355 and 2019 to about  
 356 40% and 75%,  
 357 respectively, with  
 358 the increased  
 359 number of smaller  
 360 Recreational vessels  
 361 in the database.

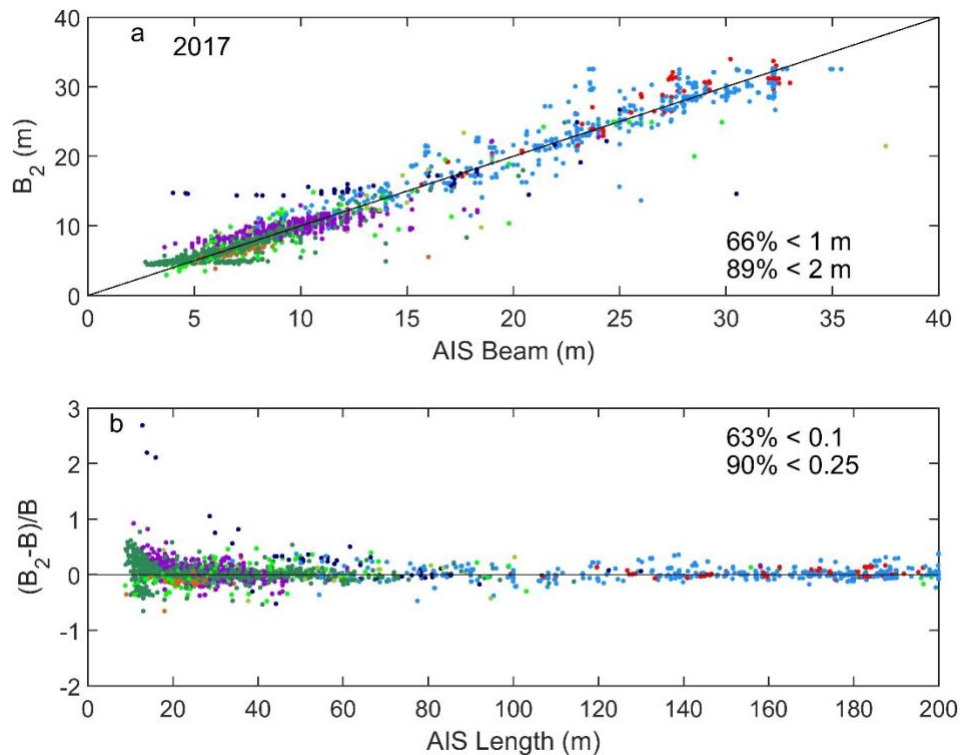


Figure 3. (a) Polynomial predicted draft ( $B_2$ ) vs AIS (from 2017) reported draft. Black line indicates the identify; (b) relative difference of estimated and reported beam vs vessel length from AIS.

362 The resulting beam  
 363 RMSD for all years  
 364 was highest (4.6 m)

365 for Supply class, with a MRAD 0.15 (Table 4). The smallest RMSD was slightly above 1 m,  
 366 found for the Fishing class, though because these vessels are smaller (maximum  $L \sim 40$  m), their  
 367 MRAD was 0.136. The smallest MRAD was found for the Tanker class at just under 0.06.

368 Differences between  $D_2$  and the AIS-reported  $D$ , followed a similar pattern. About 70% of  
 369 residuals  $\delta = |D_2 - D|$  values were  $< 1$  m and 90% were  $< 2$  m (Figure 4). The majority ( $\sim 61\%$ )  
 370 of the relative differences  $\delta/D$  were  $< 0.1$ . This was fairly consistent for the other years. The  
 371 draft RMSD for all years was largest for Cargo and Tanker ships, at  $\sim 1.4$  m. The higher number  
 372 of Cargo, Tanker, and Passenger vessels in the draft error analysis than that for beam was due to  
 373 the inclusion of  $L > 200$  m vessels in the former. Passengers ships had the lowest RMSD, just  
 374 under 0.6 m. Most of the draft MRAD were about 0.1-0.2, for all classes.

375 The polynomials (1) by definition yielded values of vessel length ( $L_{ex}$ ) that defined extrema  
 376 values of  $B$  or  $D$ , where the rate of change of the modeled variable changes sign. This was an  
 377 acceptable feature for  
 378  $L_{ex}$  outside the range  
 379 of reported  $L$  values,  
 380 or when  $L_{ex}$  was near  
 381 the range endpoints.  
 382 Most instances of  $L_{ex}$   
 383 were acceptable, but  
 384 there were some  
 385 exceptions. The most  
 386 obvious exception  
 387 being the  $D_2$  estimate  
 388 for the Tug class,  
 389 where  $L_{ex} \sim 118$  m,  
 390 with Tug lengths  
 391 ranging  $20 < L < 180$   
 392 m. This condition was  
 393 associated with a gap  
 394 in the Tug class  
 395 between  $\sim 70 < L < 150$   
 396 m, with tugs of both larger and smaller  $L$ . Tugs with  $L$  above this gap may be more appropriately  
 397 placed into a different class (e.g., Cargo), as they were generally pusher or articulated tug-barge  
 398 vessels. Future studies involving vessel classification should carefully consider both vessel type  
 399 and function.

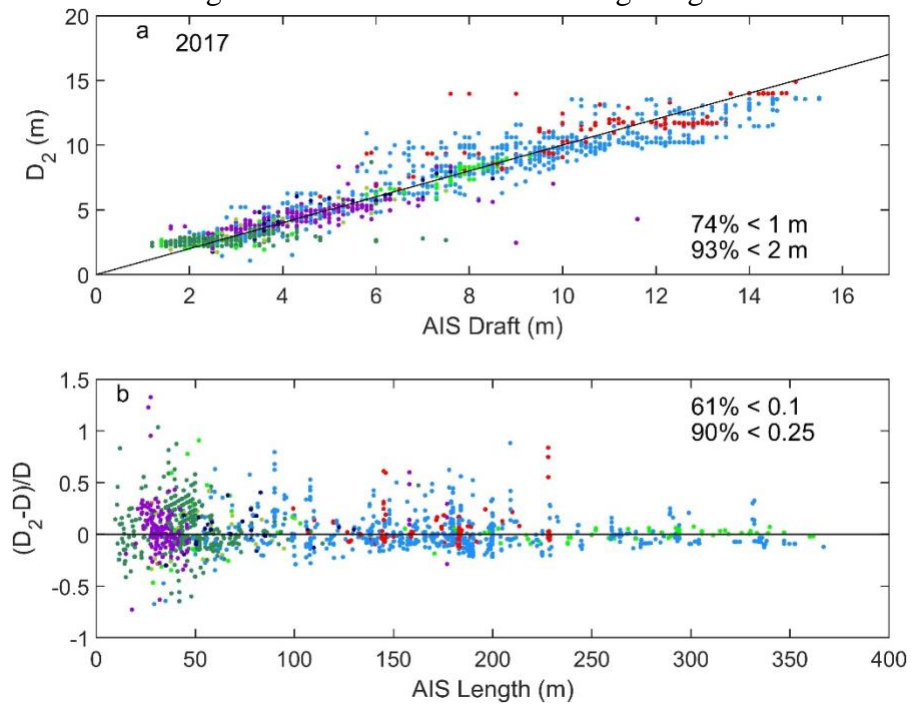


Figure 4. Same as Figure 3 but for vessel draft.

### 400 3.4 Classification

401 LR was applied as a tool for predicting the class  $c$  based on each set of  $(L, B, D)$  from AIS. Each  
 402 class was treated separately, and the  $c'$  (7) was then the set of all reports not belonging to  $c$ . The  
 403 polynomial models (Table 4) for  $B$  (with  $L < 200$  m) and  $D$  (1) for the particular  $c$  were used to  
 404 calculate residuals  $\gamma$  and  $\delta$  for all the AIS reports. The hypothesis being that vessels in  $c$  will be  
 405 distinguished by lower residuals compared to those from  $c'$ , and therefore could be usefully  
 406 modeled with LR. Reports in  $c$  were assigned  $y=1$ , and the rest  $y=0$ . The change in the  
 407 distribution of vessel beam at  $L \sim 200$  m motivated the LR models be developed in 4 cases: Case 1  
 408 included all AIS reports ( $0 < L < 400$  m); case 2 was for  $200 < L < 400$  m; cases 3 and 4 were for  
 409  $0 < L < 200$  m. Cases 1-3 used only  $\delta$  as a predictor, whereas case 4 used both  $\delta$  and  $\gamma$  as  
 410 predictors.

411 Initial attempts to build the LR models from these data frequently yielded  $p$ -values for the  $\beta$   
 412 coefficients well above 0.05, and were therefore not considered useful. This was attributed to the  
 413 unbalanced nature of the data, that is, when the ratio of the number of vessel reports in the two  
 414 sets  $n_c/n_{c'}$  was very large or very small. To eliminate this effect, the larger of the two sets were  
 415 randomly subsampled (without replacement) so that  $n_c = n_{c'}$  and the LR recalculated.

416 Rebalancing consistently yielded  
 417  $p < 0.05$  for the  $\beta$  values. Independent  
 418 subsampling of the original data was  
 419 repeated 200 times, which was  
 420 sufficient for the mean coefficient  
 421 values, denoted  $\bar{\beta}_c$ , to converge (e.g.,  
 422 Figures 5, 6). The coefficients of all the  
 423 iterations were stored, from which 95%  
 424 confidence intervals were computed  
 425 directly from the distribution of the  $\beta_c$ .  
 426 The probability of a vessel being  
 427 correctly identified to be in the “one”  
 428 class versus “the rest” was then defined  
 429 as when  $\pi(c|\delta, \gamma) \geq \pi_0(\bar{\beta}_c)$ .

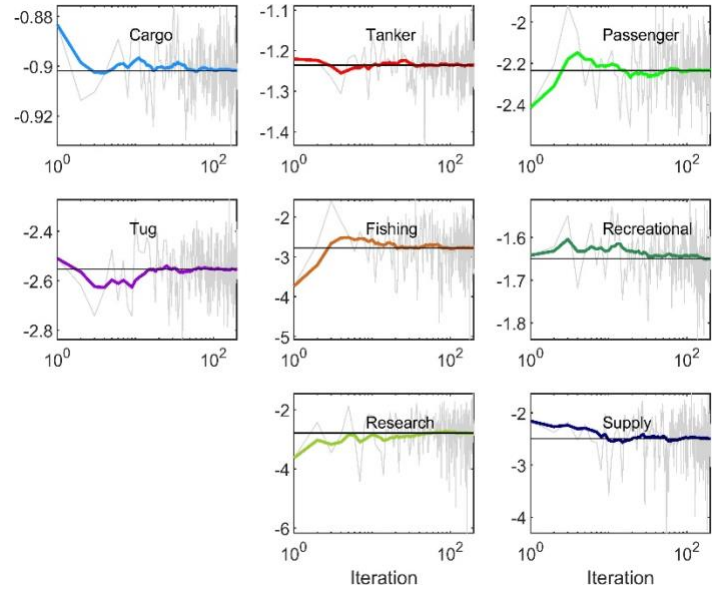


Figure 5. Case 1 constant LR coefficient for each iteration (grey), the mean value (black) and the cumulative average, for each vessel class indicated.

430 The model was tested using a limited  
 431 version of  $k$ -order cross-validation  
 432 methods (Aly, 2020; Pala and Atici,  
 433 2019). The data was divided into  $k=10$   
 434 sections of equal length. For each class in  
 435 each case, the indices within  $c$  and those  
 436 within  $c'$  were divided separately due to  
 437 the imbalance of the data. The 62 mean  
 438 coefficients computed from the  $k$  subsets  
 439 were generally close to those computed  
 440 using all the data. Relative differences  
 441 between the full-data coefficients and the  
 442 mean of the  $k$  data coefficients were  
 443 almost all small. For 57 coefficients, the  
 444 relative difference was  $< 5\%$ , with the  
 445 majority being  $< 1\%$ . The largest  
 446 exceptions to this all occurred in Case 4,  
 447 where the mean coefficient for  $B$  was  
 448 about twice that obtained in the full-data  
 449 case. The second largest deviation was for Fishing vessels, where the coefficient for  $D$  differed  
 450 from the full-data case by 10%. The relative difference of coefficients for Research vessels'

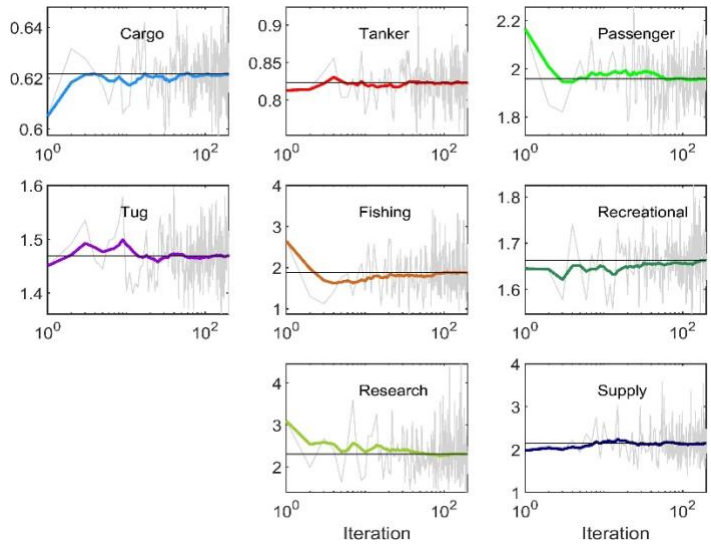
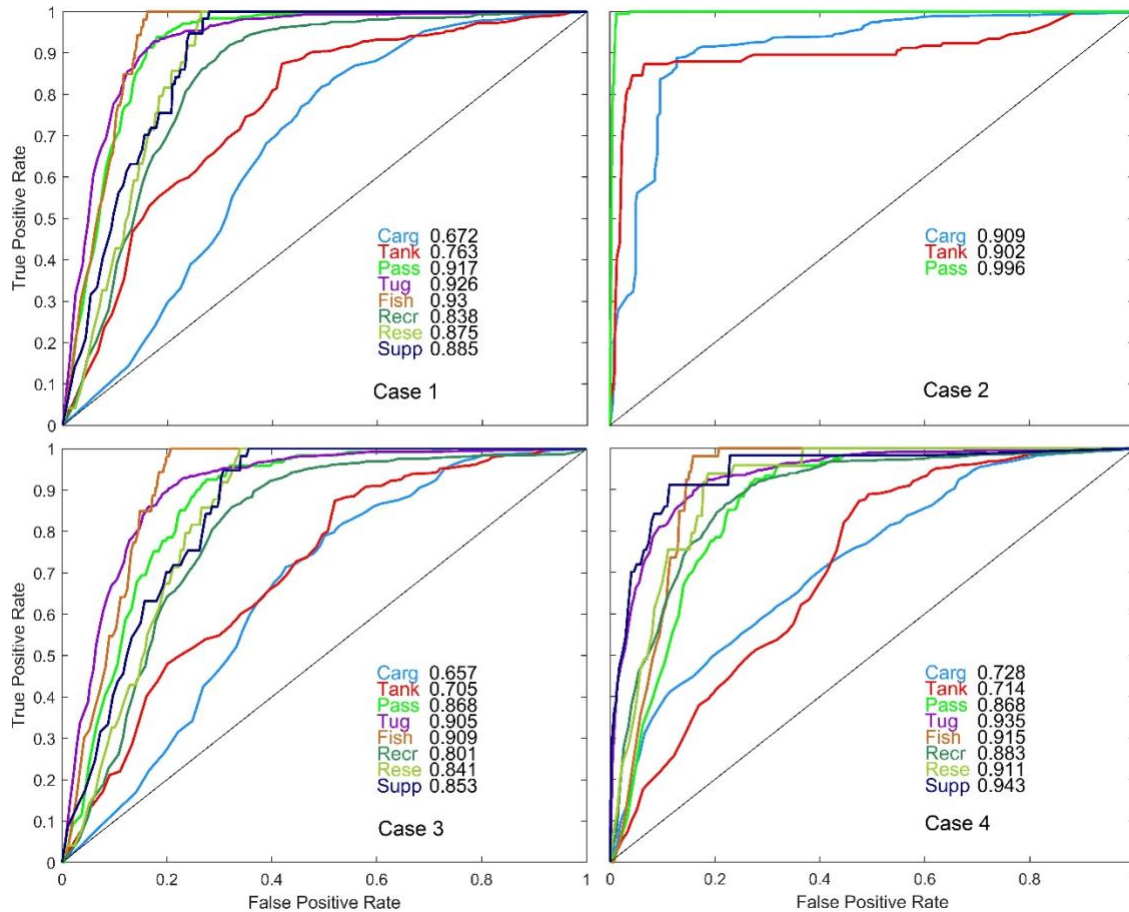


Figure 6. Same as Fig 5 but for the LR coefficient associated with the Draft variable.

451  $L, D, B$  were 6%, 7%, and 6%, respectively. There were a small number of instances where the  
 452 maximum likelihood coefficient calculation converged to a value very different from those  
 453 obtained in almost all other calculations for the same case and class. Coefficient values more  
 454 than 10 times the value obtained using all the data were discarded.



455  
 456 Figure 7. ROC curves and their AUC values for the classes (Table 1) and cases indicated. The diagonal  
 457 indicates the random classification case.

458 For all classes and cases ROC curves (Figure 7) were above the random diagonal, indicating the  
 459 results of the classification scheme was better than random. Case 1 (all vessels) had the highest  
 460 ROC curves and AUC values for Fishing, Tug, and Passenger classes, all which had an AUC >  
 461 0.9. Overall, Case 2 (large vessels) had the best results, with steeply rising curves at low FP, and  
 462 AUC values above 0.9. Case 3 yielded the lowest AUC scores for all classes, with Cargo and  
 463 Tanker classes being the worst performing with AUC of 0.657 and 0.705, respectively. All other  
 464 classes in this case had AUC > 0.8. The inclusion of a second predictor variable ( $\gamma$ ) in Case 4  
 465 raised all AUC scores compared to case 3, with Supply class rising by 0.09. Relatively large  
 466 increases also occurred in the Cargo, Recreational, and Research classes. The lowest AUC in  
 467 Case 4 was 0.714 for the Tanker class. The regression model developed for Case 1 can be

468 applied to any AIS transmission,  
 469 assuming sufficient statics are  
 470 available. Application of the other  
 471 Cases would depend on the static  
 472 values (Figure 8).

473 One way to explore the reliability of a  
 474 classification scheme is to examine the  
 475 differing characteristics of its least-  
 476 and most-confident predictions. Here,  
 477 the True Positives in Case 1 (all  
 478 vessels) were examined. Vessel  
 479 reports classified as a TP for a high  $\pi_0$   
 480 were more likely to be correctly  
 481 classified, and those satisfying low  $\pi_0$   
 482 – but not moderate or high  $\pi_0$  – were  
 483 more likely to be incorrectly classified.

484 There were two primary reasons a  
 485 vessel report might have been included  
 486 in the low confidence group: 1) the  
 487 vessel was misclassified in the AIS report, so as expected the algorithm rated it with low  
 488 probability of being a TP, and 2) a deficiency in the classification scheme, such as in the  
 489 development of the classes or misapplication of the algorithm. Examining the characteristics of  
 490 the two groups helped identify limitations of both the data set and the classification scheme.

491 The two sets of AIS reports were identified such that they exclusively define a  $TPR > 0.95$  or  $<$   
 492  $0.05$  (Figure 7), indicating low and high confidence in their classification, respectively. The  $\pi_0$  at  
 493 which these occurred varied by class. Summing over all classes, there were 487 reports in the  
 494 low confidence group, and 210 in the high confidence group. Static variables for these vessels  
 495 were then scraped from a third-party vessel traffic website, and the classification obtained was  
 496 compared to that provided in each AIS report. In the low confidence group, 53 (12%)  
 497 classifications did not match. In the high confidence group, 5 (2%) classification inconsistencies  
 498 were found. A null hypothesis that these two ratios are the same was rejected based on both chi-  
 499 squared and Fischer’s exact test well above the 99% confidence level. This further demonstrated  
 500 the method ability to detect misclassified vessels. However, the majority of reports in the low  
 501 confidence scheme were not misclassifications but large difference  $\delta$  between predicted and  
 502 reported draft.

503 The low confidence group had an average  $\delta/D_2 = 0.42$ , compared to 0.003 for the high  
 504 confidence group, indicating vessels in the former group departed from the polynomial estimated  
 505 values much more than those in the latter group. The majority of the low confidence group was  
 506 comprised of a total of 368 entries from Cargo and Tanker vessels, which, as noted above, can  
 507 have a wide variation in draft during their course of operations. The LR algorithm flagged these  
 508 with low confidence, and can be used to identify vessels operating near their extreme drafts.

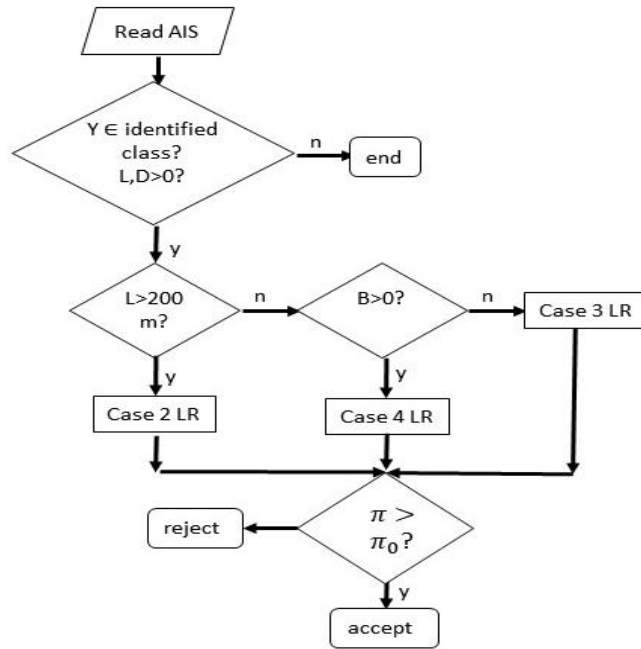


Figure 8. Schematic of vessel classification algorithm for different sets of vessel dimensions.



509 Future development should account for such normal variations of draft. The low confidence  
510 group also contained 60 Recreational and 36 Tug entries, neither of which undergo significant  
511 changes in draft during normal operations. Four of the draft values reported by the Recreational  
512 ships were roughly a factor of 3 larger than the value obtained from the third-party website, but  
513 with equal  $L$  values, suggesting these draft entries may have been in feet instead of meters. All  
514 but three of the Recreational reports had  $L < 60$  m, putting them in the area of high draft variation  
515 within their class (Figures 3 and 4). For the Tugs, 18 reported relatively small length ( $L < 50$  m),  
516 of which 13 were deeply drafted (6–10 m) pusher tugs that generally operate coupled to much  
517 longer vessels or barges. The remaining 18 Tugs reports were also deeply draft pusher or  
518 articulated tugs reporting  $L > 150$  m.

519

520

#### 521 4. Discussion

522 Erroneous or missing AIS static values are not unusual. For example, in 2019 about 21% of  
523 vessels with length  $> 30$  m operating near large Florida ports did not transmit their draft through  
524 AIS, and about 7.5% did not transmit their beam (Table 3), introducing errors in any analysis,  
525 algorithm, or operation based on the presumption the values are accurate. Here novel schemes  
526 for detecting and potentially correcting vessel beam, draft, and classification have been explored  
527 that rely on the partition of AIS types into 9 vessel classes, though not all vessels fit into the  
528 defined classes, and some vessels may better fit a class different than one indicated by their AIS  
529 type. Examples of the latter were articulated tug-barge vessels that might be more accurately  
530 classified as Tanker or Cargo vessels as their function and design is very different than the more  
531 typical (and smaller) tugs that are used to support the maneuvering of other, larger vessels. The  
532 LR classification scheme in this study demonstrated skill in verifying AIS-transmitted  
533 classification, detecting incorrectly classified vessels, and flagging those with incorrect draft or  
534 operating near an extreme draft.

535 The cornerstone of the methods presented here was the creation of independent, low-order  
536 polynomial relations between vessel length and the beam and draft for each vessel class. For both  
537  $B$  and  $D$ , over 60% of the relative differences between predicted (1) and AIS-reported values  
538 were less than 0.1, and over 90% had relative errors  $< 0.25$  (Figures 3 and 4). For many classes,  
539 these differences were due to intra-class variations in hull design, particularly for smaller Tugs  
540 and Recreational vessels. For Cargo and Tanker classes, changing deadweight was also a  
541 contributing factor to these differences. To compensate for these variations, it would be useful to  
542 create bands of values rather than simple polynomial relations. Varying the coefficients in (1)  
543 within their 95% confidence intervals would be one method to quickly develop these ranges.  
544 Using a band of acceptable values for  $B$  and  $D$  would also likely result in increased  $\pi_0$  of the  
545 True Positive rates (Figure 7).

546 Improvement of the classification scheme might also be achieved by the addition of dynamic  
547 variables such as speed, location, and turning rate, as predictor variables. For instance, it is likely  
548 a petroleum tanker will have lower draft immediately following a port call in Florida, which is  
549 not a significant petroleum producing state. Similarly, Fishing vessels are more likely to visit and  
550 remain within certain offshore areas than, say, large Cargo vessels. These examples of  
551 distinguishing vessel behavior are not sufficient to make a class determination by themselves, but  
552 could be useful in conjunction with other variables.

553 The ongoing development of corrective schemes for AIS variables suggests that these data can  
554 be treated much like some other large observational data sets, with varying levels of quality  
555 analysis and control (QA/QC). NOAA has an extensive procedure for QA/QC of real-time  
556 oceanographic measurements (Hofmann and Healy, 2017), with older instrument types such as  
557 tide gauges having more robust protocols than newer instruments such as chemical sensors.  
558 Possible levels of QA/QC for AIS are outlined as follows:

559 Level 0: raw, decoded AIS data, directly readable in the form of text, csv, or similar formats. No  
560 correction applied.

561 Level 1: Vessels would be identified using their reported MMSI, and possibly their IMO number,  
562 name, and other identifying information (Winkler, 2012). Missing or suspect static variables  
563 would be replaced with values taken from the historical records of the identified vessel. The  
564 existence of such records is assumed, so this would be best applied to vessels of sufficient age to  
565 generate the proper database. This level could also include removal and correction of isolated  
566 anomalous dynamic values such as large spikes in velocity or position. Precautions would need  
567 to be implemented in cases of erroneous MMSI, when the same MMSI is reported for different  
568 vessels, or when a vessel changes its MMSI as sometimes occurs when coming under new  
569 ownership.

570 Level 2: Interpolative schemes would be used to fill missing static values for vessels without  
571 records sufficient to permit application of Level 1 corrections. The schemes would be developed  
572 using sets of related vessel types. The polynomial relations developed here provide an example,  
573 where vessels were organized into functional classes and the (presumably correct) length and  
574 class were used to estimate beam and draft. It would be instructive to develop these relations on  
575 much larger sets of vessels as it is possible some bias was introduced in the selection of Florida  
576 as a test bed. With a sufficient number of vessels, it may be possible to create interpolative  
577 methods for each AIS type. Other groupings of vessels might yield different results, but  
578 constraints of nautical design necessitate a limited ranges of hull geometries (Figure 2). Multi-  
579 hull designs such as catamarans and trimarans would likely need to be treated separately.

580 Level 3: AI/ML methods would synthesize the full AIS record, including both static and  
581 dynamic variables, of the individual vessel and other vessels, to detect and correct errors and  
582 omissions in AIS reports. Some initial steps towards developing such a set have been taken using  
583 corrected AIS position records (Masek et al., 2021). Level 3 might also include use of data

584 beyond the AIS, such as Synthetic Aperture Radar (SAR) and optical imaging from low-orbiting  
585 satellites to determine ship class, size and speed (Purivigraipong, 2018; Riveiro et al., 2018),  
586 stationary mounted cameras, local radar, or similar instruments placed onto aircraft (Eaton et al.,  
587 2018). The addition of *B* to the predictor set increased the AUC values of some classes by ~0.1  
588 (Figure 7), suggesting the addition of other predictors could further increase the accuracy of the  
589 classification scheme. The number of useful predictors is likely to be limited by the “curse of  
590 dimensionality” (Geenens, 2011) where the calculation of model parameters (e.g.,  $\beta$ ) fails to  
591 converge due to a sample space made sparse by the inclusions of too many independent  
592 variables.

593 The AIS provides essential information for the management and control of maritime operations,  
594 is widely used in retrospective studies of vessel activities, and in the ongoing transformation of  
595 the maritime industry by artificial intelligence and related technologies (Artikis and Zissis, 2021;  
596 de la Peña Zarzuelo et al., 2020; Plaza-Hernández et al., 2020). The methods described here  
597 provide a new method for detecting and potentially updating some static AIS variables,  
598 supporting these efforts.

## 599 **Acknowledgments**

600 This research was made possible in part through a cooperative agreement between NOAA’s  
601 Office of Coast Survey and the University of South Florida through the Center for Ocean  
602 Mapping and Innovative Technologies (COMIT) (Award #NA20NOS4000227), the NOAA  
603 IOOS Program Office as sub-awards through the Southeast Coastal Ocean Observing Regional  
604 Association (Award #NA16NOS0120028, Sub-Award #IOOS.16(028)USF.ML.OBS.1 and  
605 IOOS.16(028).USF.ML.GAPS MINIPROPOSAL.5), and the Gulf of Mexico Coastal Ocean  
606 Observing System (Award #NA16NOS0120018, Sub-Award #02-S160275), and from the  
607 Greater Tampa Bay Marine Advisory Council-PORTS, Inc. (Award #2500-1066-00).

608

609

610

## 611 LITERATURE CITED

612

613 Aly, H.H., 2020. A novel approach for harmonic tidal currents constitutions forecasting using hybrid  
614 intelligent models based on clustering methodologies. *Renewable Energy* 147, 1554-1564.

615 Artikis, A., Zissis, D., 2021. *Guide to Maritime Informatics*. Springer Nature.

616 Bertram, V., Schneekluth, H., 1998. *Ship design for efficiency and economy*. Elsevier

617 Bisong, E., 2019. *Logistic Regression, Building Machine Learning and Deep Learning Models on Google  
618 Cloud Platform*. Springer, pp. 243-250.

619 Bošnjak, R., Šimunović, L., Kavran, Z., 2012. Automatic identification system in maritime traffic and error  
620 analysis. *Transactions on maritime science* 1 (02), 77-84.

621 Chen, P., Shi, G., Liu, S., Gao, M., 2018. Pattern Knowledge Discovery of Ship Collision Avoidance based  
622 on AIS Data Analysis. *International Journal of Performability Engineering* 14 (10).

623 de la Peña Zarzuelo, I., Soeane, M.J.F., Bermúdez, B.L., 2020. Industry 4.0 in the port and maritime  
624 industry: A literature review. *Journal of Industrial Information Integration*, 100173.

625 Demšar, U., Vrřrantaus, K., 2010. Space–time density of trajectories: exploring spatio-temporal patterns  
626 in movement data. *International Journal of Geographical Information Science* 24 (10), 1527-1542.

627 Dobrkovic, A., Iacob, M.-E., van Hillegersberg, J., Mes, M.R., Glandrup, M., 2016. Towards an approach  
628 for long term AIS-based prediction of vessel arrival times, *Logistics and Supply Chain Innovation*.  
629 Springer, pp. 281-294.

630 Eaton, R.S., German, S., Balasuriya, A., 2018. Maritime Border Security using Sensors, Processing, and  
631 Platforms to Detect Dark Vessels, 2018 IEEE International Symposium on Technologies for Homeland  
632 Security (HST). IEEE, pp. 1-5.

633 Elhassan, T., Aljurf, M., 2016. Classification of imbalance data using torek link (t-link) combined with  
634 random under-sampling (rus) as a data reduction method. *Global J Technol Optim S* 1.

635 Emmens, T., Amrit, C., Abdi, A., Ghosh, M., 2021. The promises and perils of Automatic Identification  
636 System data. *Expert Systems with Applications* 178, 114975.

637 Fawcett, T., 2006. An introduction to ROC analysis. *Pattern Recognition Letters* 27 (8), 861-874.

638 Geenens, G., 2011. Curse of dimensionality and related issues in nonparametric functional regression.  
639 *Statistics Surveys* 5, 30-43.

640 Guo, H., Wei, T., 2019. Logistic regression for imbalanced learning based on clustering. *International*  
641 *Journal of Computational Science and Engineering* 18 (1), 54-64.

642 Guo, S., Mou, J., Chen, L., Chen, P., 2021. An Anomaly Detection Method for AIS Trajectory Based on  
643 Kinematic Interpolation. *Journal of Marine Science and Engineering* 9 (6), 609.

644 Harati-Mokhtari, A., Wall, A., Brooks, P., Wang, J., 2007. Automatic Identification System (AIS): Data  
645 Reliability and Human Error Implications. *Journal of Navigation* 60 (3), 373-389.

646 Harre, I., 2000. AIS adding new quality to VTS systems. *The Journal of Navigation* 53 (3), 527-539.

647 Hilbe, J.M., 2016. Practical guide to logistic regression. CRC Press.

648 Hofmann, C., Healy, J., 2017. Real-time quality control experiences using QARTOD in Australian ports.  
649 *Australasian Coasts & Ports 2017: Working with Nature*, 612.

650 Hosmer Jr, D.W., Lemeshow, S., Sturdivant, R.X., 2013. Applied logistic regression. John Wiley & Sons.

651 Huang, J., Ling, C.X., 2005. Using AUC and accuracy in evaluating learning algorithms. *IEEE Transactions*  
652 *on Knowledge and Data Engineering* 17 (3), 299-310.

653 Jahn, C., Scheidweiler, T., 2018. Port Call Optimization by Estimating Ships' Time of Arrival, *International*  
654 *Conference on Dynamics in Logistics*. Springer, pp. 172-177.

655 King, G., Zeng, L., 2001. Logistic regression in rare events data. *Political analysis* 9 (2), 137-163.

656 Klimaszewski, J., 2015. A comparison of regularization techniques in the classification of handwritten  
657 digits. *Journal of Theoretical and Applied Computer Science* 9 (4), 3-7.

658 Lim, G.J., Cho, J., Bora, S., Biobaku, T., Parsaei, H., 2018. Models and computational algorithms for  
659 maritime risk analysis: a review. *Annals of Operations Research*, 1-22.

660 Liu, B., 2015. Maritime Traffic Anomaly Detection from Ais Satellite Data in Near Port Regions, *Computer*  
661 *Science*. Dalhousie University, p. 91.

662 Masek, M., Lam, C.P., Rybicki, T., Snell, J., Wheat, D., Kelly, L., Smith-Gander, C., 2021. The open  
663 maritime traffic analysis dataset.

664 Merlo, J., Chaix, B., Ohlsson, H., Beckman, A., Johnell, K., Hjerpe, P., Råstam, L., Larsen, K., 2006. A brief  
665 conceptual tutorial of multilevel analysis in social epidemiology: using measures of clustering in  
666 multilevel logistic regression to investigate contextual phenomena. *Journal of Epidemiology &*  
667 *Community Health* 60 (4), 290-297.

668 Meyers, S.D., Luther, M.E., Ringuet, S., Raulerson, G., Sherwood, E., Conrad, K., Basili, G., 2020.  
669 Characterizing Vessel Traffic Using the AIS: A Case Study in Florida's Largest Estuary. *Journal of*  
670 *Waterway, Port, Coastal, and Ocean Engineering* 146 (5), 05020005.

671 Mitchell, K.N., Scully, B., 2014. Waterway performance monitoring with automatic identification system  
672 data. *Transportation Research Record* 2426 (1), 20-26.

673 Murk, D.W., 1999. Vessel traffic management: a new philosophy, Proceedings of the Marine Safety  
674 Council, Washington, DC.

675 Oh, J.-Y., Kim, H.-J., Park, S.-K., 2018. Detection of ship movement anomaly using AIS data: a study.  
676 *Journal of Navigation and Port Research* 42 (4), 277-282.

677 Pala, Z., Atici, R., 2019. Forecasting Sunspot Time Series Using Deep Learning Methods. *Solar Physics* 294  
678 (5), 50.

679 Papanikolaou, A., 2014. Ship design: methodologies of preliminary design. Springer.

680 Plaza-Hernández, M., Gil-González, A.B., Rodríguez-González, S., Prieto-Tejedor, J., Corchado-Rodríguez,  
681 J.M., 2020. Integration of IoT Technologies in the Maritime Industry, International Symposium on  
682 Distributed Computing and Artificial Intelligence. Springer, pp. 107-115.

683 Purivigraipong, S., 2018. Review of Satellite-Based AIS for Monitoring Maritime Fisheries. *ENGINEERING*  
684 *TRANSACTIONS* 21 (1), 44.

685 Riveiro, M., Pallotta, G., Vespe, M., 2018. Maritime anomaly detection: A review. *Wiley Interdisciplinary*  
686 *Reviews: Data Mining and Knowledge Discovery* 8 (5), e1266.

687 Robards, M., Silber, G., Adams, J., Arroyo, J., Lorenzini, D., Schwehr, K., Amos, J., 2016. Conservation  
688 science and policy applications of the marine vessel Automatic Identification System (AIS)—a review.  
689 *Bulletin of Marine Science* 92 (1), 75-103.

690 Rong, H., Teixeira, A., Soares, C.G., 2019. Ship trajectory uncertainty prediction based on a Gaussian  
691 Process model. *Ocean Engineering* 182, 499-511.

692 Salas-Eljatib, C., Fuentes-Ramirez, A., Gregoire, T.G., Altamirano, A., Yaitul, V., 2018. A study on the  
693 effects of unbalanced data when fitting logistic regression models in ecology. *Ecological Indicators* 85,  
694 502-508.

695 Shelmerdine, R.L., 2015. Teasing out the detail: How our understanding of marine AIS data can better  
696 inform industries, developments, and planning. *Marine Policy* 54, 17-25.

697 Sheng, K., Liu, Z., Zhou, D., He, A., Feng, C., 2018. Research on Ship Classification Based on Trajectory  
698 Features. *Journal of Navigation* 71 (1), 100-116.

699 Sidibé, A., Shu, G., 2017. Study of automatic anomalous behaviour detection techniques for maritime  
700 vessels. *The Journal of Navigation* 70 (4), 847-858.

701 Silveira, P., Teixeira, A., Soares, C.G., 2013. Use of AIS data to characterise marine traffic patterns and  
702 ship collision risk off the coast of Portugal. *The Journal of Navigation* 66 (6), 879-898.

703 Smestad, B.B., Asbjørnslett, B.E., Rødseth, Ø.J., 2017. Expanding the possibilities of ais data with  
704 heuristics.

705 Son, G.M., Choi, W.J., Baek, J.E., Shin, D.W., Yang, C.S., 2022. Approach to Classifying Ship Types from AIS  
706 Data Using DNN and CNN, ISRS 2022 (International Symposium on Remote Sensing 2022). ISRS, pp. 242-  
707 244.

708 Steidel, M., Lamm, A., Feuerstack, S., Hahn, A., 2019. Correcting the Destination Information in  
709 Automatic Identification System Messages. Springer International Publishing, Cham, pp. 496-507.

710 Stivaktakis, R., Tsagkatakis, G., Moraes, B., Abdalla, F., Starck, J.-L., Tsakalides, P., 2019. Convolutional  
711 neural networks for spectroscopic redshift estimation on euclid data. *IEEE Transactions on Big Data* 6 (3),  
712 460-476.

713 Sun, Y., Chen, X., Jun, L., Zhao, J., Hu, Q., Fang, X., Yan, Y., 2021. Ship trajectory cleansing and prediction  
714 with historical ais data using an ensemble ann framework. *Int. J. Innov. Comput. Inf. Control* 17, 443-  
715 459.

716 Tu, E., Zhang, G., Rachmawati, L., Rajabally, E., Huang, G.-B., 2017. Exploiting AIS data for intelligent  
717 maritime navigation: A comprehensive survey from data to methodology. *IEEE Transactions on*  
718 *Intelligent Transportation Systems* 19 (5), 1559-1582.

719 Wang, Y., Yang, L., Song, X., Li, X., 2021. Ship classification based on random forest using static  
720 information from AIS data, *Journal of Physics: Conference Series*. IOP Publishing, p. 012072.  
721 Wang, Y., Zhang, J., Chen, X., Chu, X., Yan, X., 2013. A spatial–temporal forensic analysis for inland–water  
722 ship collisions using AIS data. *Safety Science* 57, 187-202.  
723 Winkler, D., 2012. AIS Data Quality and the Authoritative Vessel Identification Service (AVIS). National  
724 GMDSS Implementation Task Force, Arlington, VA.  
725 Xin, X., Liu, K., Yang, X., Yuan, Z., Zhang, J., 2019. A simulation model for ship navigation in the  
726 “Xiazhimen” waterway based on statistical analysis of AIS data. *Ocean Engineering* 180, 279-289.  
727 Yang, D., Wu, L., Wang, S., Jia, H., Li, K.X., 2019. How big data enriches maritime research—a critical  
728 review of Automatic Identification System (AIS) data applications. *Transport Reviews*, 1-19.  
729 Zhang, P., Zhu, D.-x., Leng, W.-h., 2008. Parametric approach to design of hull forms. *Journal of*  
730 *Hydrodynamics*, Ser. B 20 (6), 804-810.  
731 Zhao, L., Shi, G., Yang, J., 2018. Ship trajectories pre-processing based on AIS data. *The Journal of*  
732 *Navigation* 71 (5), 1210-1230.  
733 Zhou, Y., Daamen, W., Vellinga, T., Hoogendoorn, S., 2019. Review of maritime traffic models from  
734 vessel behavior modeling perspective. *Transportation Research Part C: Emerging Technologies* 105, 323-  
735 345.  
736 Zhu, J., Hastie, T., 2004. Classification of gene microarrays by penalized logistic regression. *Biostatistics* 5  
737 (3), 427-443.

738

739

740 Figure Captions

741 Figure 1. Map of peninsular Florida. The 5 largest ports are indicated.

742 Figure 2. (a) Unique-vessel beam vs length, by functional class (Table 1). Dashed lines indicate  
743 Panamax beam (PX) and Post-Panamax (PPX) beam sizes. Number of vessels ( $N$ ) with both  
744  $L, Y > 0$  and  $0 < B \leq 200$  m is indicated. (b) Unique-vessel draft vs length, coded by functional  
745 class. Solid lines are quadratic fits for each class. Number of vessels with  $L, D, B, Y > 0$  is  
746 indicated.

747 Figure 3. (a) Polynomial predicted draft ( $B_2$ ) vs AIS (from 2017) reported draft. Black line indicates the  
748 identify; (b) relative difference of estimated and reported beam vs vessel length from AIS.

749 Figure 4. Same as Figure 3 but for vessel draft.

750 Figure 5. Case 1 constant LR coefficient for each iteration (grey), the mean value (black) and the  
751 cumulative average, for each vessel class indicated.

752 Figure 6. Same as Fig 6 but for the LR coefficient associated with the Draft variable.

753 Figure 7. ROC curves and their AUC values for the classes (Table 1) and cases indicated. The diagonal  
754 indicates the random classification case.

755